Transition from tungsten erosion to carbon layer deposition with simultaneous bombardment of tungsten by helium and carbon

Ivan Bizyukov

Kharkiv National University, Faculty of Physics and Technologies, 31 Kurchatov Ave.,
Kharkiv 61108, Ukraine

Karl Krieger

Max-Planck-Institut für Plasmaphysik, EURATOM Association, Boltzmannstr. 2,
85748 Garching, Germany

Abstract

Simultaneous bombardment of tungsten layers with helium and carbon ions leads to both erosion of tungsten and implantation of carbon. The underlying processes have been investigated numerically and experimentally as a function of the carbon fraction in the incident ion flux for ion energies in the keV range. Tungsten layers were deposited on polished single crystal silicon substrate by magnetron sputter deposition to eliminate the influence of surface roughness on the experimental results. The fluence dependent dynamics of the surface composition was measured *in-situ* by ion beam analysis. The given projectile-target system is subject only to kinematic processes and is therefore particularly suitable for benchmarking of purely kinematic simulations based on the binary-collision approximation, like implemented in the TRIDYN code. TRIDYN calculations match the experimental results very well, which demonstrates the validity of the kinematic description. In particular the simulations allow to predict the change of surface composition by bombardment with gaseous and non-volatile ions, as well as the transition point from W erosion to C deposition as function of the carbon fraction in the incident ion flux.

Keywords: simultaneous ion bombardment, carbon implantation, tungsten sputtering, transition point.

1. Introduction

In the design of the International Tokamak Experimental Reactor (ITER), tungsten (W) will be used for plasma-facing components (PFCs) in the divertor baffle region, which are exposed to high particle and heat fluxes [1, 2, 3]. Complete coverage of the first wall with tungsten is envisaged in future reactor devices because of the unsurpassed life-time of tungsten based PFCs. Experience with W PFCs in the ASDEX Upgrade tokamak has shown that W is sputtered mainly by multiply charged low-Z impurities, which can be accelerated in the sheath potential to energies of up to several keV [4]. In ITER low-Z impurities will be migrating to W surfaces due to erosion of the beryllium (Be) main wall and of the carbon (C) based divertor target plates. Complicated sputtering and deposition effects are expected for both elements. Carbon is of particular relevance for the W PFCs at the divertor baffle area as it is eroded in significant amounts at the adjacent divertor target plates and after being ionized in the plasma can migrate to the W surfaces. C bombardment of W can lead not only to W sputtering but also to the formation of C layers, which significantly affect both sputtering and the formation of fuel inventories [5, 6, 7].

Simultaneous bombardment of the W surface with gaseous and C ions strongly influences the competition between erosion of the surface and deposition of C layers. The surface composition is determined by the balance between implantation and sputtering of C and at the same time influences sputtering rates of the elements contributing to the mixed material. The complicated interdependency between surface composition and ion-surface interactions, as well as its impact on the transition point between continuous W erosion and continuous C layer growth requires experimental validation of numerical simulations based on the binary collision approximation. However, there is a certain problem in the study of simultaneous bombardment of W surfaces with deuterium (D) and C ions, since this projectile combination is further complicated by formation of hydrocarbons and their chemical sputtering [8, 9]. This process generally leads to an increase of the sputtering yield of W atoms from mixed surfaces, but is not taken into account by kinematic codes like TRIDYN [10]. Since there are no quantitative experimental data on the contribution of the hydrocarbon formation to W sputtering, the comparison between simulation and experiment can not be interpreted unambiguously. Therefore, the modeling should be validated by a projectile-target system, which is subject only to kinematic processes.

In this case the kinematic processes determine directly the transition point from steady-state surface erosion to continuous growth of a C layer. Although the balance between sputtering and implantation has been intensively studied in the past few years, there is still no complete understanding of the underlying processes and there is as yet no clear definition for the transition point available. We define the transition point by a set of parameters (flux, ion species energy, incidence angles, species ratio, *etc.*) of the steady-state interaction between the incident flux including the gaseous and non-volatile ions and the mixed surface. An infinitely small shift of any of these parameters will result in a transition from steady-state erosion to continuous growth of a C layer (and vice versa). The prediction of the transition point is of particular interest for fusion devices because it separates areas of continuous erosion from areas which will become covered by re-deposited material.

As an example of a projectile-target system subject only to kinematic processes, this work describes experiments and simulations of the simultaneous bombardment of W surfaces with helium (He) and C ions and the dependence of erosion and implantation processes on the C fraction in the total incident flux, particularly with respect to the transition from W erosion to C layer growth. He is the lightest gaseous noble element and therefore its kinematic interaction with C and W is expected to be similar to D excluding chemical effects. As surface roughness may critically affect the ion-surface interaction for low energies and light projectiles, W layers were deposited on Si mono-crystal polished wafers instead of using bulk tungsten samples. It has been shown in previous experiments that W layers on Si wafer substrate provide a sufficiently smooth surface to exclude roughness effects on the erosion and implantation processes [7].

2. Experimental

The experiments were performed with mass-separated 12 keV C_2^- and 3 keV He^+ ions with energies chosen to obtain maximum beam flux densities. It is assumed that each C projectile atom has a fractional incidence energy of 6 keV. The angle of incidence for both species is 15°. Ion beam analysis (IBA) with 2.5 MeV ^{3}He ions was performed *in-situ* between bombardment steps, monitoring the evolution of surface composition with increasing fluence. A key advantage of using IBA methods is the capability to detect the transition from dynamic surface changes to steady-state, which can not be detected by weight-loss measurements due to the large difference between the masses of W and C atoms.

The use of W layers as a bombarded sample allows to use Rutherford back-scattering (RBS) for the measurement of the W areal density with an accuracy of 1%. The change of W areal density is calculated from the difference between the initial and the post-bombardment values. The main potential error source would be the uncertainty of the stopping power, which, however, cancels out as the decrease of the areal density is measured relatively to the initial value.

Key point of the experimental technique is the additional ability to detect the amount of implanted C, which can be also used for the validation of the model. The amount of implanted C was measured using the nuclear reaction ^{12}C(^{3}He,p)^{14}N [11]. These measurements were evaluated using a reference a-C:D layer with known D and C areal densities with a resulting accuracy <10%. Further details of the experimental setup, as well as of the measurement technique are described in [12].

The W layers (thickness ≈260±30 nm) were deposited by magnetron sputter deposition onto Si single crystal wafers with an intermediate cupper (Cu) layer (thickness ≈380±40 nm) in the same process. The intermediate Cu layer was introduced as a marker for RBS measurements. Further details on structure and properties of the samples can be found in [13]. X-ray photoelectron spectroscopy was used to quantify the low-Z impurity content of the layers to fractions of carbon, oxygen and nitrogen <1%. The thickness of the W layer was chosen to be large enough to prevent any interaction of the projectiles and recoils with the layers below. The mean projectile ranges of 6 keV C and 3 keV He are $R_C \approx 10$ nm and $R_{He} \approx 14$ nm respectively, depending on surface composition. Average roughness of W layer is $R_a \approx 14$ nm and it is comparable to projectile ranges of the ions. Since $R_a \approx R_C$, R_{He}, the sample surface can be assumed smooth and the effect of surface roughness can be neglected [7].

3. Results and discussion

Each experiment was performed at a fixed C fraction in the total incident flux f_C, therefore, different values of f_C correspond to different experiments with each bombardment starting with a pure surface. According to previous measurements the relative concentration of He in tungsten is expected to be ≈10% [14], which is small in comparison to the concentrations of W and C atoms. Therefore, the evolution of the surface composition was simulated neglecting He retention.

3.1. Evolution of surface composition

Depending on the C fraction in the incident flux, the dynamical change of the surface composition can be divided in the two scenarios described in section 1, characterized as steady-state sputtering of the surface and continuous C layer growth respectively. The evolution of the surface composition typical for the first scenario is presented in Figure 1, (a) and (b). Figure 1(c) shows in addition the long term stability of the set value of f_C, which was obtained from current measurements. Small deviations of the f_C value from the set average value still may result in corresponding deviations of the measured C areal density from simulation results (see subsection

3.3 below). However, short term excursions of f_C (spikes in Figure 1(c)) do not lead to any observable deviation.

Figure 1(a) shows that the evolution of the C areal density on the surface shows a similar behavior in case of the steady-state sputtering scenario: an initial growth of implanted C saturates at a certain level above a fluence of typically 2×10^{18} cm^{-2}. The saturation value of the C areal density is monotonically increasing as function of f_C. The steady-state sputtering scenario is additionally characterized by a constant composition of the implantation zone, which is independent of fluence. In this scenario the flux of implanted C is balanced by the flux of sputtered and reflected C resulting in the observed constant elemental composition of the surface. Figure 1(a) shows a C contamination of the virgin surface in the range of 10^{16} cm^{-2}, which explains the observed deviation of the experimental data from the simulation at low fluence in the case of f_C=3%.

Apart from the stationary surface composition, the sputtering yield should also remain constant after reaching steady-state. However, both the experimental and calculated decrease of the W areal density are nearly linear from the beginning of the ion bombardment within the experimental error (Figure 1(b)). The linear decrease of the W areal density shows that the correspondingly constant sputter yield, is not significantly influenced by the formation of the mixed W-C surface. More detailed consideration of the sputtering dynamics shows that the available measurement methods are not sensitive enough to reveal the expected minor change of the sputter yield in the initial bombardment phase. For example, at f_C=15% the calculated initial sputter yield is $Y_W \approx 0.12$, decreasing to $Y_W \approx 0.073$ after reaching steady-state (Figure 2(a)). This drop of the sputter yield results in a change of the initial decrease of W areal density (Figure 2(b)) below the detection threshold. The predicted deviation of the initial sputter yield from the steady-state value is also comparable to the scatter of experimental points and can therefore not be detected.

If f_C reaches a certain threshold, the initial growth of implanted C is no longer balanced by re-erosion and continuously increases until the surface is ultimately covered by a C layer (with a fraction of implanted He). Figure 3 shows the computed dynamics of the C areal density for f_C=24% and f_C=25%. One can see, that the C areal density is still turning stationary at a fluence of $>5\times10^{18}$ cm^{-2} for f_C=24%. In contrast, a continuous increase of the C areal density is predicted for f_C=25%, which is synonym to continuous growth of a C layer. Therefore, the transition point for the given system and given projectile parameters is in the interval $24\% < f_C < 25\%$. The evolution of surface composition has been experimentally studied with f_C=21% and f_C=24%.

In contrast to the predicted continuous erosion scenario, Figure 4 shows already an evolution of the surface composition typical for the second scenario of continuous C layer growth. However, one observes also a much larger deviation of the measured dynamics from the computed one (Figure 4, (a) and (b)). These deviations can be explained in case of f_C=21% by strong drops of f_C in the experiment, while the experiment with f_C=24% was performed without instability of the beam currents. The results clearly show that the experimental accuracy does not allow an exact determination of the transition point due to the diverging fluence to reach equilibrium. In addition, in the case of continuous C layer growth the effects of implanted He can no longer be neglected. In contrast, because of the absence of gaseous ions, the growth of a pure C layer by bombardment of a W surface with C ions can be excellently predicted by TRIDYN [7].

3.2. Parametric representation of the evolution

The parametric representation of the erosion-implantation equilibrium with the use of implantation-sputtering curves introduced in [7] shows the evolution of the surface composition in the parameter space spanned by “continuous W sputtering” and “continuous C implantation”. This representation of the experimental and simulation results should more clearly reveal any disagreement, since it naturally excludes the effect of experimental errors originating from the calculation of the projectiles absolute fluence. Excluding such errors is important because in case of simultaneous irradiation with two species, the experimental data still retain errors originating from fluctuations of the respective beam fluxes leading to fluctuations of the C/He ratio in the total incident flux. The parametric representations of the data in Figure 1 and Figure 4 are shown in Figure 5.

Figure 5(a) shows the implantation-sputtering curves for the case f_C=3%, 9% and 15%. It again confirms the accuracy of the TRIDYN simulations as long as f_C is away from the critical value. The decrease of the number of W atoms in W layer due to sputtering is accompanied by an increasing amount of implanted C atoms. Small deviations of the experimental data from the simulations can be explained by fluctuations in time of the local f_C value at the IBA measurement position due to fluctuations of the magnetic field in the mass separation magnets. In case of f_C=3%, one can observe the influence of the initial impurity contamination of the surface on the dynamical part of the surface composition evolution as already discussed in subsection 3.1. The initial amount of carbon correspondingly decreases the fluence required for reaching steady-state sputtering.

The good agreement between experimentally obtained and simulated implantation-sputtering curves shows that the local C/He ratio at the ion beam analysis area can be derived from integral current measurements with sufficient accuracy. Previous experiments with single beam bombardment [7, 13] have also shown that experimental errors in the determination of local fluence values are sufficiently small that significant deviations of experimental data from simulation curves are not expected.

At higher values of f_C, the evolution of the surface composition turns to a continuous build up of a C layer that appears as a monotonic increase of the C areal density (Figure 5(b)). Figure 5(b) shows that f_C=21% is very close to or already on the “continuous C deposition” side of the transition point. From comparison to the corresponding simulations one can infer that the transition point can be predicted with an accuracy of <10%.

3.3. *Ion-surface interactions at steady-state*

As it has been shown above, the evolution of surface composition during bombardment with He and C ions is of non-linear process. However, after reaching steady-state in the continuous W erosion scenario, ion-surface interactions can be described by two values independent on fluence:

- Areal density of implanted C retained within the projectile ion range.
- Sputtering yield of W, Y_W. It can be calculated as $Y_W = \frac{\Delta W}{\Delta \Phi}$, where ΔW is areal density of W atoms, sputtered by ions, which fluence is $\Delta \Phi$.

These values can be obtained by both experiment and simulation. Experimentally, the areal density of C implanted at steady-state was derived from the average over the last several values.

Experimentally, steady-state sputtering was observed up to f_C=18%. Each point in Figure 6 has been obtained as a result of a separate bombardment of a virgin W layer starting at zero fluence and reaching steady-state. W erosion and C implantation for a given f_C value were obtained simultaneously in the same experiment. Both, experimental results and simulation show that the amount of C retained at steady-state increases with f_C, until it gets close to the transition point. The simulation results show the increase in the slope of the curve, which will diverge at the transition point (Figure 6(a)). The disagreement between experiment and theory slowly increases towards higher f_C values.. This is expected because of the divergence of the slope towards the transition point, which in turn leads to large changes of the amount of implanted C at a relatively small increase of the f_C value. One should note, that uncertainties in the fluence measurement do not enter this comparative analysis, since at steady-state the amount of implanted C on the surface depends only on the C/He ion ratio in the incident flux.

In contrast to the nearly linear growth of the amount of implanted C with f_C , experimental values of the sputtering yield Y_W show small fluctuations around the constant Y_W value in the studied range of f_C (Figure 6(b)). The experiment shows also a ≈30% higher W sputtering yield than calculated by TRIDYN. This can still be considered as a good agreement for this kind of measurements. The variation of the sputter yield calculated by TRIDYN in the given range is still of the same magnitude than the fluctuations of the experimentally determined Y_W values. The most likely source of the observed disagreement is the inaccuracy of the fluence measurement. Furthermore, one observes that the non-linear increase of implanted C corresponds to a drop of Y_W in simulations, which can be attributed to the strongly decreasing concentration of W atoms on the surface towards the transition point.

A linear growth of Y_W , as plotted with dots in Figure 6(b), would only occur if the W sputtering yield was independent of the elemental composition of the mixed surface. In other words, the sputtering rate of W atoms Y_W in that case would be determined only by the fraction of the contributing ion species in the total incident flux (f_C or f_{He}):

$$Y_W = f_C Y_W^C + f_{He} Y_W^{He},$$

where Y_W^C and Y_W^{He} are sputtering yields of pure W due to C and He ion impact respectively. This approach is often used for fast calculations of the sputtering yields in impurity transport calculations for fusion plasmas. However, Figure 6(b) shows that neglecting the modification of the elemental composition can lead to large errors in the simulation of W sputtering by simultaneous impact of volatile and non-volatile elements.

4. Conclusions

W layers were bombarded simultaneously in the IPP Garching dual ion beam facility with ions of He and C. The kinematic properties of this system are close to those of the system D+C → W, while at the same time excluding possible chemical interactions between implanted species that may significantly contribute to sputtering. The influence of surface roughness could be excluded by the use of W layers with smooth surfaces on the length scale of ion implantation range. Therefore, the studied system was very well suited for benchmarking simulations with

Monte-Carlo codes based on the binary collision approximation. The elemental surface composition was studied as a function of incident fluence and its dynamics was studied as a function of the C fraction in incident flux f_C .

Comparison of experimental results and simulations has revealed a good agreement, so the model of ion-surface interactions has shown to be valid for the case of simultaneous bombardment with gaseous and non-volatile ions. The model particularly well describes the dynamical change of the surface composition, as well as steady-state characteristics of ion-surface interactions, as long as f_C was well below the critical value denoting the transition from continuous W erosion to continuous C implantation. The increasing disagreement with increasing f_C value, was, however, always reasonably small taking into account uncertainties in the fluence measurements. The transition point (defined by a critical f_C value) has been predicted by the simulations with an accuracy of ≈10%. The most likely source of disagreement between experiment and simulation is the neglect of He implantation and its retention in the near surface region in the simulations. The results of both experiments and simulations demonstrate that sputtering of materials by simultaneous impact of gaseous and non-volatile elements can not be described by just assuming a linear superposition of the sputter yields of the contributing ion species.

Acknowledgements

The authors would like to thank Dr. A . Gigler for AFM measurements; P. Matern, G. Matern, S. Lindig, M. Fusseder, J. Dorner for valuable technical assistance.

References

[1] G. Janeschitz, ITER JCT and ITER HTs, J. Nucl. Mat. vol. 290-293 p.1 (2001).

[2] D. Meade, et al., Mission and design of the fusion ignition research experiment, in: Proceedings of the 18th IAEA Conf. on Fusion Energy, Sorrento, Italy October, 2000, (CD-ROM), pp. IAEA-CN-77/FTP2/16, IAEA, Vienna, 2001.

[3] S. Nishio, et al., Conceptional design of advanced steady-state tokamak reactor, in: Proceedings of the 18th Conf. on Fusion Energy, Sorrento, Italy October, 2000, (CDROM), pp. IAEA-CN-77/FTP2/14, IAEA, Vienna, 2001.

[4] K. Krieger et al., J. Nucl. Mat. Vol.266 –269 p.207 (1999).

[5] W.Eckstein, J.Roth, Nucl. Instrum. and Methods in Phys. Res., vol.B83, p.279 (1991).

[6] K. Schmid, J. Roth. J. of Nucl. Mat. Vol. 302 p.96–103 (2002).

[7] I. Bizyukov, K. Krieger, N. Azarenkov, U. von Toussaint, J. Appl. Phys. Vol.100, 113302 (2006).

[8] W. Eckstein, K. Krieger, J. Roth, J. Nucl. Mat. Vol.258-263 p.912-916 (1998).

[9] K.Schmid, J.Roth, J. of Nucl. Mat. vol.313 –316 p.302 –310 (2003).

[10] W. Moeller, W. Eckstein, J.P. Biersack, Comput. Phys. Commun. Vol.51 p.355 (1988).

[11] S.Y. Tong, W.N. Lennard, P.F.A. Alkemada, I.V. Mitchell, Nucl. Instrum. Methods B45 (1990) 41

[12] I. Bizyukov, K. Krieger. Rev. Sci. Instrum. 77 (2006) 043501

[13] I. Bizyukov, K. Krieger, N. Azarenkov, S. Levchuk, Ch. Linsmeier, J. Nucl. Mat. 337-339 (2005) 965.

[14] H.T. Lee, A.A. Haasz, J.W. Davis and R.G. Macaulay-Newcombe. J. Nucl. Mater. Vol. 360 p. 196-207 (2007)

List of figure captions

Figure 1. Fluence dependent surface and incident flux parameters for f_C values of 3%, 9% and 15%: (a) – change of C areal density due to implantation; (b) – decrease of W areal density in bombarded layer due to sputtering; (c) – alteration of C fraction in total incident flux.

Figure 2. Simulated sputter yield of tungsten (a) and decrease of W areal density in the layer as function of incident fluence. Open circles correspond to simulated values. The solid line represents a linear fit of the steady-state decrease of W areal density at f_C=15%.

Figure 3. Fluence dependent C areal density at steady-state surface sputtering (f_C=24%) and continuous C layer growth (f_C=25%) simulated by TRIDYN.

Figure 4. Fluence dependent surface and incident flux parameters close to transition point for cases of 21% and 24%: (a) – change of C areal density due to implantation; (b) – decrease of W areal density in bombarded layer due to sputtering; (c) – alteration of C fraction in total incident flux.

Figure 5. Implantation-sputtering curves for cases of (a) – f_C=3%, 9%, 15%; (b) – f_C=21% and 24%.

Figure 6. Parameters of steady-state ion-surface interaction as function of the C fraction in the total incident flux, f_C: (a) – areal density of C implanted; (b) – sputter yield of W.

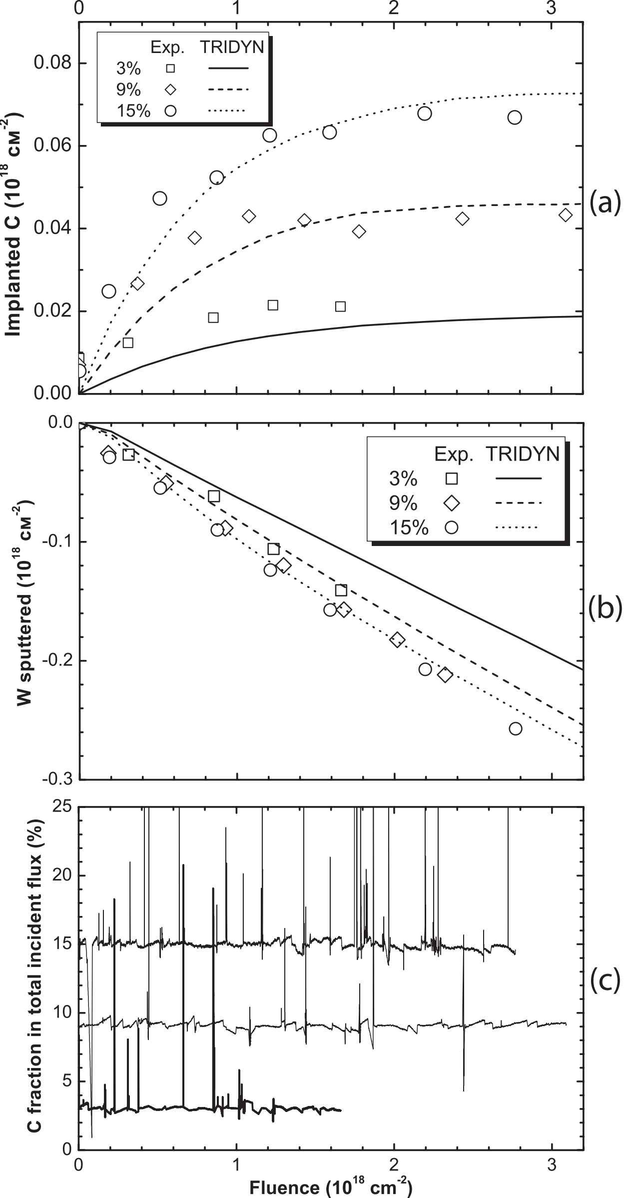

0
1
2
3
Exp.
TRIDYN
3%
9%
15%
Implanted C (10^{18} cm^{-2})
0.00
0.02
0.04
0.06
0.08
(a)
W sputtered (10^{18} cm^{-2})
0.0
-0.1
-0.2
-0.3
Exp.
TRIDYN
3%
9%
15%
(b)
C fraction in total incident flux (%)
0
5
10
15
20
25
(c)
0
1
2
3
Fluence (10^{18} cm^{-2})

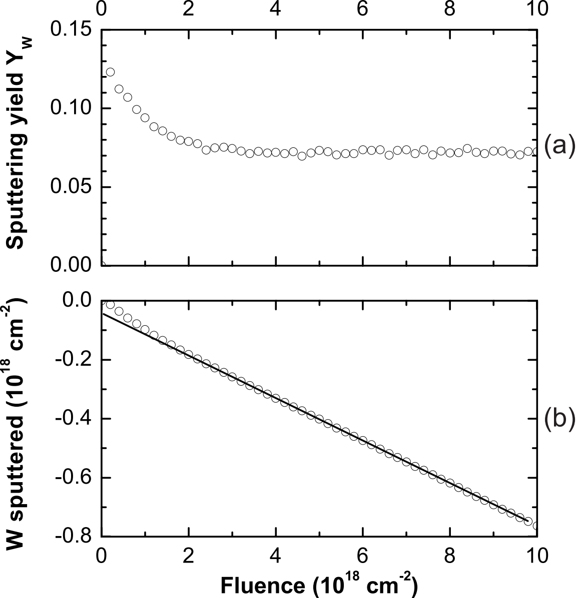
0
2
4
6
8
10
0.15
0.10
0.05
0.00
Sputtering yield Y_W
(a)
0.0
-0.2
-0.4
-0.6
-0.8
W sputtered (10^{18} cm^{-2})
(b)
0
2
4
6
8
10
Fluence (10^{18} cm^{-2})

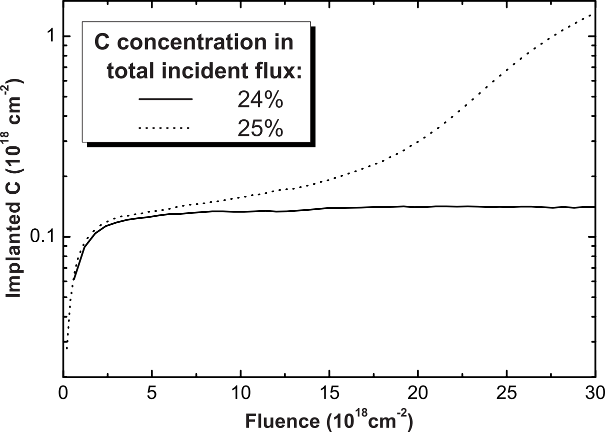
C concentration in total incident flux:
24%
25%
Implanted C (10^{18} cm^{-2})
1
0.1
Fluence (10^{18}cm^{-2})
0
5
10
15
20
25
30

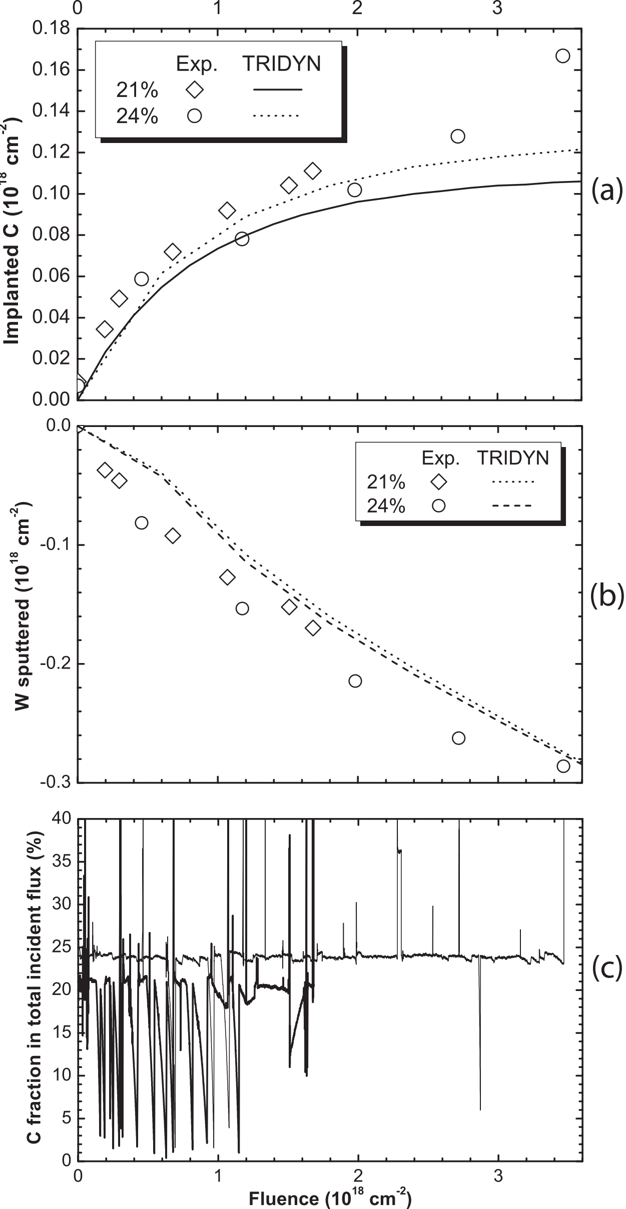
0
1
2
3
0.18
0.16
0.14
0.12
0.10
0.08
0.06
0.04
0.02
0.00
Implanted C (10^{18} cm^{-2})
Exp.
TRIDYN
21%
24%
(a)
0.0
-0.1
-0.2
-0.3
W sputtered (10^{18} cm^{-2})
Exp.
TRIDYN
21%
24%
(b)
40
35
30
25
20
15
10
5
0
C fraction in total incident flux (%)
(c)
0
1
2
3
Fluence (10^{18} cm^{-2})

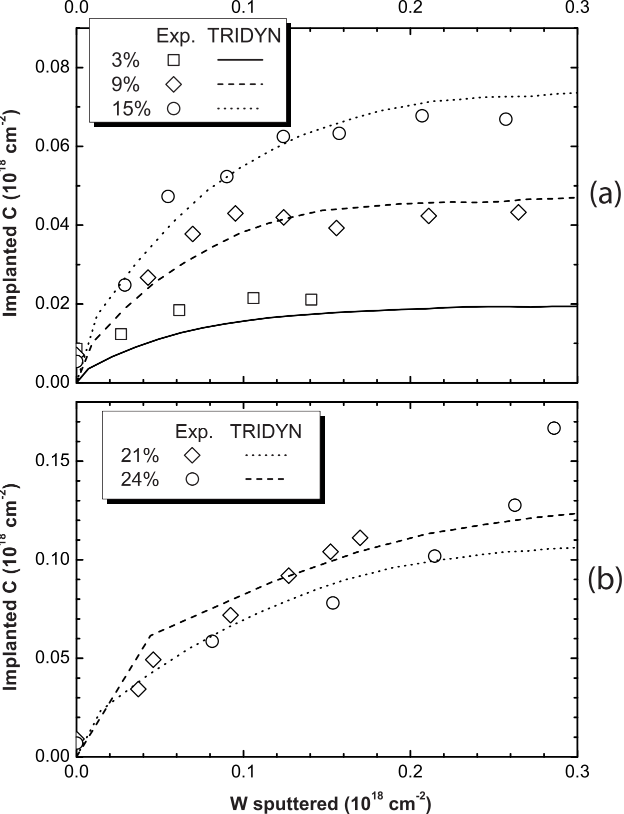
0.0
0.1
0.2
0.3
Exp.
TRIDYN
3%
9%
15%
0.08
0.06
0.04
0.02
0.00
Implanted C (10^{18} cm^{-2})
(a)
Exp.
TRIDYN
21%
24%
0.15
0.10
0.05
0.00
Implanted C (10^{18} cm^{-2})
(b)
0.0
0.1
0.2
0.3
W sputtered (10^{18} cm^{-2})

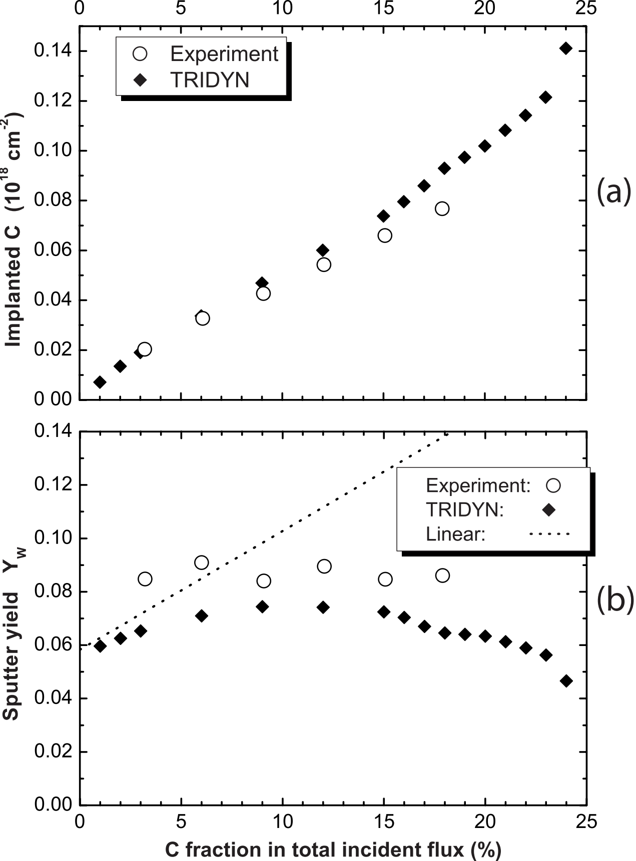
(a)
Experiment
TRIDYN
Implanted C (10^{18} cm^{-2})
0.14
0.12
0.10
0.08
0.06
0.04
0.02
0 00
0
5
10
15
20
25
(b)
Experiment:
TRIDYN:
Linear:
Sputter yield Y_W
0.14
0.12
0.10
0.08
0.06
0.04
0.02
0.00
0
5
10
15
20
25
C fraction in total incident flux (%)